AD 703 272

LASER DAMAGE STUDY OF THIN FILMS

Arthur F. Turner, et al

Bausch and Lomb, Incorporated
Rochester, New York

28 February 1970

DEPARTMENT OF THE NAVY

OFFICE OF NAVAL RESEARCH

WASHINGTON, D. C. 20360

RESEARCH AND DEVELOPMENT

BAUSCH & LOMB INCORPORATED

ROCHESTER, NEW YORK 14602

CONTRACT NO. N00014-68-C-0190 MOD. P002

LASER DAMAGE STUDY OF THIN FILMS

EIGHTH and FINAL QUARTERLY REPORT

FOR THE PERIOD

29 November 1969 to 28 February 1970

[illegible]

LASER DAMAGE STUDY OF THIN FILMS

Contract No.	N00014-68-C-0190 MOD. P002
Order No.	ARPA Order 306
Name of Contractor	Bausch & Lomb Incorporated Rochester, New York 14602
Date of Contract	1 September [redacted] 1967
Amount of Contract	$65,492.00
Contract Expiration Date	28 February 1970
Project Scientist	Dr. A. F. Turner (716) 232-6000 Ext. 296

EIGHTH and FINAL QUARTERLY REPORT

Report Prepared By: E. Arlin and A. F. Turner

For the Period: 29 November 1969 to 28 February 1970

ABSTRACT

Damage thresholds for evaporated ZrO_2 films and multilayers, in combination with MgF_2 films, were determined using a Q-switched ruby laser. Antireflection and beam divider coatings as well as high reflecting quarterwave stacks were represented in the multilayers tested. Threshold values lie in the 30-40 J/cm^2 range for coatings with up to 15 layers. Beyond this the thresholds decrease. The CO_2 laser assembled here was improved by introducing O-ring seals for the Brewster windows and by more efficient water cooling. It is stable at 60 W multimode for periods of hours. Semi-quantitative observations were made on metal films of several thicknesses - Ag, Cu, Al, Au and Inconel. Au appears most damage resistant. Inconel films show promise for photographic recording at 10.6 μm.

TABLE OF CONTENTS

LIST OF FIGURES

INTRODUCTION

During this contract's 8th and final quarter the work was divided between dielectric film damage measurements with the ruby laser (Spaceray 101C) and semi-quantitative observations on metal film damage with the CO_2 laser constructed in this laboratory. Accordingly this report is divided into three sections:

I. Ruby Laser Damage Thresholds in Multilayers

II. CO_2 Laser Operation with Observations on Metal Film Damage

III. Two-Year Contract Summary

SECTION I

RUBY LASER DAMAGE THRESHOLDS IN MULTILAYERS

1.0 Choice of Film Materials

Previous work on this contract, reported during the 6th Quarter, 1 December 1968 - 28 February 1969, had indicated high threshold values for several ZrO_2/MgF_2 multilayer film combinations. It appeared important to verify this in a more systematic manner, especially since ZrO_2 is nonabsorbing as far as 240nm in the ultraviolet and thus, in combination with MgF_2 which also has a high threshold and is transparent to much shorter wavelengths, offers the possibility of making damage resistant coatings over a significant portion of the ultraviolet spectrum as well as in the visible and near infrared. Four principal types of coatings were studied, namely single ZrO_2 films, beam dividers, monochromatic antireflection coatings and high reflecting quarterwave stacks. All of these are of interest in laser equipment.

2.0 Coating Constructions

General comments on each coating as well as measured examples of their spectrophotometric curves are given in what follows. In the coating formulations H stands

for a quarterwave film of ZrO_2 and L for a quarterwave film of MgF_2, each with respect to some reference wavelength λ_o which must be chosen in practice to position the spectrophotometric features in the desired part of the spectrum. G stands for the glass substrate, A for air.

2.1 Single Films GHA

Measurements of the reflectance of single quarterwave films are used to derive their refractive index. Glass of index 1.52 coated on one side with a quarterwave ZrO_2 film reflects about 25% from which a film index of 2.06 follows. The dispersion throughout the visible spectrum is small.

2.2 Beam Divider GLHA (with GHLA for comparison of thresholds)

Glass of index 1.52 coated on one side with GLHA reflects 28.6% and can be useful as a beam divider, Figure 1. Samples of the reverse construction GHLA also were tested for possible differences in threshold, Table 2.

2.3 Monochromatic Antireflection Coating GHH(.9L)A (with GHLA for comparison)

The simple antireflection coating GHHLA has a symmetrical reflectance curve with two equal minima as shown in Figure 2A. Using ZrO_2 and MgF_2 films, if the

latter is made 10% thinner than a quarterwave, i.e., GHH(.9L)A, then the short wavelength minimum rises, while the long wavelength minimum approaches zero. Thus the asymmetric construction affords an efficient monochromatic antireflection coating. In Figure 2B the measured reflectance at λ = .694 was .04%.

For a comparison of thresholds, samples with the construction GHLA were made under the same coating conditions, with the results given below in Paragraph 6.0.

2.4 Quarterwave Reflecting Stacks

6 Layer	G $(LH)^3$A	(#1)
15 Layer	G $(HL)^7$HA	(#3)
21 Layer	G $(HL)^{10}$HA	(#2)

Stacks of quarterwave films find use as optical cavity coatings and a choice of reflectances is often convenient. By means of a shutter arrangement in the vacuum coater it was a simple matter to make several stacks in one coating cycle. The procedure was to use three substrates on the work holder behind a shutter such that piece #2 was always open whereas #1 was closed with #3 open and vice versa. The coating operation on pieces #2 and #3 was interrupted after the 15th layer, the shutter closed over #3 and opened over #1, and the 21-layer coating then completed

on piece #2. There resulted the three stacks indicated above.

Figure 3 gives the measured curves of samples of three such stacks from transmittance measurements with a Cary Model 14 Spectrophotometer. Since the coatings are essentially free of absorption, 1 - T = R. On this basis for the 6-layer stack the peak reflectance is 71%, for the 15-layer stack it is 97.8%, and for the 21-layer stack the reflectance peaks at 99.7%.

The threshold determinations for these and miscellaneous other stacks are given in Paragraph 7.0.

3.0 Vacuum Coaters

The film samples were produced in two different laboratory coaters. #1 is a 48" horizontal tank coater with a 16" oil diffusion pump. #2 is a 30" box coater with a 10" oil diffusion pump. #1 was operated in the 1 to 3 x 10^{-4}Torr pressure range for both the MgF_2 and ZrO_2, with no deliberate gas bleed-in. #2 was operated at a pressure of 1 to 2 x 10^{-5}Torr for the MgF_2. For the ZrO_2 oxygen was bled in to raise the pressure to 1 x 10^{-4}Torr. In #1 coater the substrates were held at 125°C during the coating deposition, in #2 coater they were held at 315°C. Since the damage thresholds were consistently

higher for the samples from coater #2 the results in the tabulations to follow are grouped according to the coater used.

4.0 Damage Thresholds for Single Quarterwave Films of ZrO_2 and MgF_2

In the tables to follow the damage threshold values J_t in joules are listed for the individual samples tested. These J_t values are obtained by extrapolating to zero radius a plot of incident joules vs. radius of damage according to a routine method developed here in the course of this work and described in several previous reports, e.g., Quarterly Report for the Period 1 October 1966 - 31 December 1966 on Contract NONR-4717(00). The laser beam was always incident on the coated side of the substrate.

The thresholds J_t in joules are converted to thresholds E_t in joules cm^{-2} by multiplying by an instrumental constant which was determined to be $780cm^{-2}$ for the equipment used. In the tables the threshold energies J_t are averaged before converting to threshold energy densities E_t. The display of the individual energy thresholds is informative of the large scatter encountered, which is probably to be expected since we are dealing with a specialized

strength-of-materials problem. In general the number of samples was not large enough to carry out a meaningful statistical analysis.

4.1 Quarterwave ZrO_2 Films

Table 1 gives the thresholds for ZrO_2 films with quarterwave positions throughout the wavelength range 300-700nm. These positions are not specified since no trend with wavelength was evident.

Table 1

Measured Thresholds J_t in Joules and
Average Thresholds E_t in Joules cm^{-2}.

Single Quarterwave Films GHA

G = 1.52 Glass H = QW ZrO_2

A = Air

#1 Coater		#2 Coater			
Run	J_t	Run	J_t	Run	J_t
313	.022	C-591-1	.036	C-592-1	.020
315	.021	-2	.040	-2	.019
316	.026	-3	.047	-3	.040
317	.026	-4	.033	-4	.028
AV.	.024 J		.039 J		.027 J
E_t	19 Jcm^{-2}		30.5 Jcm^{-2}		21 Jcm^{-2}

4.2 Comments on Table 1 Results

In #2 coater the substrates were held at much higher temperatures than in #1 coater (315°C vs. 125°C), and an O_2 bleed was used. These factors probably cause the significantly higher thresholds in samples from #2 coater.

4.3 Quarterwave MgF_2 Films

From previous contract work, e.g., the preceding 7th Quarterly Report for the period 1 September to 28 November 1969, it is known that for quarterwave MgF_2 films:

$$E_t = 45 \text{ Jcm}^{-2}$$

5.0 Beam Divider Thresholds

As mentioned in Paragraph 2.2 the MgF_2/ZrO_2 film combination GLHA provides a plate beam divider reflecting about 29%, see Figure 1. Such samples were tested in comparison with the reversed combination GHLA and the results are contained in Table 2.

Table 2

Measured Thresholds J_t in Joules and

Average Thresholds E_t in Joules cm^{-2}

GLHA Beam Dividers vs. GHLA

G = 1.52 Glass H = QW ZrO_2

A = Air L = QW MgF_2

Run	GLHA J_t	#2 Coater GHLA J_t
C-587	--	.068
C-588	.019	.037
C-595	.027	.046
C-596	.034	.039
C-597	.055	.046
AV.	.034 J	.047 J
E_t	27 Jcm^{-2}	37 Jcm^{-2}

5.1 Comments

Not only did the GHLA sequence have the higher threshold, the appearance of its damage areas was also quite different. The top MgF_2 film splits away from the bottom ZrO_2 film over a wide circle around the damage nucleus. Consequently its damage curve in Figure 4 is much steeper than that for the GLHA construction. It has generally been observed

that relatively steep damage curves are associated with an explosive type of damage. The high tensile stresses in MgF_2 films may be a factor here.

6.0 Two Layer Antireflection Coating Thresholds

A very effective monochromatic antireflection coating can be made starting with the common halfwave/quarterwave combination and making adjustments on the thickness of the quarterwave component. As described in Paragraph 2.3 a reflectance near zero can be obtained at one wavelength with a ZrO_2/MgF_2 combination if the MgF_2 is made 10% thinner than a quarterwave, see Figure 2B.

Table 3 lists the experimental threshold determinations on a series of these antireflection coatings, designated GHHLA for simplicity, in comparison with GHLA combinations made under like coating conditions.

Table 3

Measured Thresholds J_t in Joules and

Average Thresholds E_t in Joules cm^{-2}

GHHLA Antireflection Coatings vs. GHLA

G = 1.52 Glass   H = QW ZrO_2

A = Air   L = QW MgF_2

	#1 Coater			#2 Coater		
	GHHLA		GHLA		GHHLA	GHLA
Run	J_t	Run	J_t	Run	J_t	J_t
282	.024	286	.023	601	.054	.045
300	.019	301	.028	602	.054	.049
308	.020	309	.031			
310	.016	311	.024			
325	.014	312	.018			
326	.018					
330	.021					
AV	.019 J		.025 J		.054 J	.047 J
E_t	15 Jcm^{-2}		19.5 Jcm^{-2}		42 Jcm^{-2}	37 Jcm^{-2}

6.1 Comments on Table 3 Results

The strong dependence of threshold values on the coating technique is here in evidence more than in Table 1. The thresholds are more than doubled by having the substrates very hot and bleeding O_2 during the ZrO_2 coating operation (see Paragraph 3.0). Figure 5 shows typical damage curves.

7.0 Quarterwave Multilayer Stack Thresholds

Because of their importance as high reflecting coatings for optical cavities a rather extensive study was made of the thresholds of multilayer ZrO_2/MgF_2 quarterwave stacks. The results for samples from #1 coater are shown in Table 4, and from #2 coater in Table 5. With the shuttering equipment in #2 coater a series of three stacks, with 6, 15 and 21 layers, was made in each coating cycle, as explained in Paragraph 2.4. Measured reflectance curves are given in Figure 3. In #1 coater all stacks made in a single pump-down had the same number of layers.

Measured Thresholds J_t in Joules and
Average Thresholds E_t in Joules cm^{-2}

11, 13 and 15-Layer Quarterwave Stacks

$G\ (HL)^5 HA$ $G\ (HL)^6 HA$ $G\ (HL)^7 HA$

G = 1.52 Glass H = QW ZrO_2
A = Air L = QW MgF_2

#1 Coater

Run	11-Layer J_t	13-Layer J_t	15-Layer J_t
278	.022		
279		.029	
273			.022
274			.035
275			.026
285			.024
304			.021
307			.029
AV	.022 J	.029 J	.026 J
E_t	17 Jcm^{-2}	23 Jcm^{-2}	20 Jcm^{-2}

Table 5

Measured Thresholds J_t in Joules and

Average Thresholds E_t in Joules cm^{-2}

6, 15 and 21-Layer Quarterwave Stacks

$G\ (LH)^3 A \qquad G\ (HL)^7 HA \qquad G\ (HL)^{10} HA$

G = 1.52 Glass   H = QW ZrO_2

A = Air   L = QW MgF_2

#2 Coater

Run	6-Layer J_t	15-Layer J_t	21-Layer J_t
C-594	.020	.028	.020
C-599	.056	.045	.041
C-603	.058	.028	.019
C-604	.041	.036	.028
C-605	.044	.025	.019
AV	.044 J	.032 J	.025 J
E_t	34 Jcm^{-2}	25 Jcm^{-2}	19.5 Jcm^{-2}

7.1 Comments on Table 4 and 5 Results

A comparison of the tables again shows that the coating techniques employed in #2 coater produce the higher threshold values. Damage curves from a series of three quarterwave stacks made in it are given in

Figure 6. Moreover it was found that with #1 coater the stacks were limited to 15 layers. More layers resulted in coating breakdown.

As with the TiO_2/SiO_2 stacks described in the 7th Quarterly Report, here too the damage craters had stepped sides, the number of steps being half the number of layers in the stack. This observation is suggestive of an action of the standing wave pattern within the stack since the loops of the pattern fall at alternate interfaces.

Of especial interest in Table 5 is the decline in threshold values with increasing number of layers, and hence with increasing reflectance. The threshold ratios for the 6, 15 and 21-layer stacks are as 1.8:1.3:1 with the reflectance ratios being as .7:.98:1.00 (see Figure 3). Thus the threshold ratios are inversely as the reflectance ratios, contrary to what one might a priori conclude, since a high reflectance might be expected to "protect" the interior of the stack from damage. The explanation might simply be that thin film coatings tend to become structurally weaker as the number of layers is increased, due to the inherent mechanical stresses which develop in them as well as for other reasons, such as an increase in the number of imperfections. Also a finite amount

of absorption in the film materials would be cumulative. However, the decrease in threshold values with increasing stack reflectance may also be further qualitative evidence of the role of the standing wave pattern within the quarterwave structure in contributing to the damage mechanism. As the number of layers is increased the standing wave patterns become more pronounced, the excursions of the E vector at the loops become greater and the electrostrictive and other such disruptive effects at the alternate interfaces grow. The stepped nature of the damage craters would seem to corroborate this explanation.

8.0 Summary

Single ZrO_2 films and simple multilayers in combination with MgF_2 films can be expected to have damage thresholds for ruby laser radiation in the range 30 to 40 Jcm^{-2} when made under optimum conditions. Above about 15 layers the threshold values decline, becoming about 20 Jcm^{-2} for 21-layer quarterwave stacks.

SECTION II

CO_2 LASER AND DAMAGE TO THIN METAL FILMS

The CO_2 laser has obtained a maximum output of 60 watts $\pm$ 2%. Power densities of up to 2.2 kw/cm^2 have been utilized to study minimum power densities needed to damage thin metal films of Ag, Cu, Al, Au and inconel.

1.0 The CO_2 Laser (Figure 7)

The CO_2 laser construction was described in the 5th Quarterly Report for the period 1 September to 30 November, 1968. The operating conditions and preliminary observations of damage to metals were described in the 7th Quarterly Report, 1 September to 28 November, 1969.

Improvements in design, reliability and output power have been made and are as follows.

1.1 The NaCl windows have been mounted on a Brewster window mount of new design (Figure 8). This design consists of an Al block which was cut at the Brewster andle on one end and flat on the other, with an inside bore of one inch. The inds were then machined for rubber O-ring seals. These O-ring seals were used to hold the polished NaCl crystal at the Brewster angle. The mount was also held to the Corning 1½"

I.D. pipe by these seals. The O-ring allowed the NaCl window to expand or contract with respect to the mount and thus eliminated the danger of breakage due to a differential thermal expansion between the Brewster mount and the NaCl window. Also, the Brewster window mounts allowed easier alignment of the laser and quick replacement of the windows.

1.2 A heat exchange system was installed to facilitate cooling of the discharge tube. The water ballast was kept at a temperature of 12°C. The heat exchange system greatly improved the power output of the laser.

1.3 The Germanium output mirror was held in a water-cooled mount made of Cu. The optical cavity mirrors used during this contract period had the following characteristics:

Output Mirror:	Ge with $R_1 = \infty$, $R_2 = \infty$. 1.750" diameter. Antireflected at 10.6 μm to less than 2% on one side and 80% reflectivity on the other. Purchased from Coherent Radiation Laboratories.
End Mirror:	Glass 1/8 diopter (R_1=16m). Ophthalmic ground curve. Opaque Au coated.

1.4 The gas mixture consisted of 80% He, 10% N_2 and 10% CO_2. The pressure was from 7 to 10 Torr. The gases were introduced into the cavity by the use of separate valve controls. The current drain at these pressures was 80-100 MA at 15-16 KV.

These design improvements have led to an increase in maximum power output and stability. The laser is now capable of 60 W $\pm$ 2% in a multimode operation for long periods of time (at least 4 hrs.) and 25 W $\pm$ 2% in a TEM_{00} mode of operation.

2.0 CO_2 Laser Damage to Metal Coatings

High power densities (2.2 KW/cm^2) were achieved by focusing a 61 W/cm^2 beam to .025 cm^2. This was done with a Au coated short focal length mirror (f=10 cm). These high power densities were then used to test the minimum power density needed to damage Inconel, Ag, Cu, Al, and Au.

2.1 Preparation of Coatings

Figures 9, 10, 11 and 12 show the relationship of percent reflectance and transmittance data at .6328 μm and at 10.6 μm vs. film thickness for Ag, Cu, Al and Au. These plots allow a convenient correlation between film transmittance and reflectance at 10.6 μm and at a monitoring wavelength of .6328 μm in the vacuum coater.

Au, Cu, Al and Inconel were evaporated by resistance heating using three .1-inch tungsten rods arranged as a "log raft". Ag was evaporated by resistance heating using a corrugated tantalum strip.

2.2 Damage to Inconel

Inconel was considered "damaged" when a decrease in optical density was just detectable, presumably due to re-evaporation from the substrate. The results of power density "damage" studies on different percent transmittance Inconel films can be found in a plot of time vs. W/cm^2 vs. percent transmittance at .6328 μm (Fig. 13). This plot indicates that Inconel (a high nickel alloy, optical constants at 10.6 μm unknown) was easily re-evaporated from glass. The higher the transmittance, the faster it evaporated or the lower the power necessary for it to evaporate.

Due to the ease with which a thin Inconel film changes in optical density when submitted to low power, and the way it shows an imprint of the mode structure of the laser, when running multimode, it is felt that Inconel on glass may be used as a form of photographic recording plate for 10.6 μm radiation.

2.3 Damage to Au

The experimentation on Au was done by varying four parameters. (1) The power density was varied between 30 W/cm^2 and 2 KW/cm^2. (2) The transmittance of the film at .6328 μm was varied from 7% to 52%. (3) The substrates used were 1.52 index glass, KBr, NaCl and BaF. (4) The length of time was varied during which the film was exposed to the power densities mentioned above.

The results of the experiments on Au films are as follows. The Au films themselves were not damaged for power densities below 1.3 KW/cm^2, but the substrates of KBr, BaF and glass cracked at these power levels. NaCl substrates were not damaged. At 2 KW/cm^2, Au films broke down on glass. A CrAuCr film on glass was also destroyed at a power density of 2 KW/cm^2.

2.4 Damage to Al.

An Al film opaque at .6328 μm was damaged at about 50 W/cm^2 in a few seconds. This damage seems to have been caused by heating. The Al melted and then formed into beads.

2.5 Damage to Ag

Slightly cloudy or dirty opaque Ag films were destroyed by a power density of 2.26 KW/cm^2. Clean Ag films were damaged at this power density only after a much longer exposure (about a minute). Thus, heating of

the substrate, due to absorption of the 10.6 μm radiation, had a great deal of effect in destroying the films.

2.6 Damage to Cu

Cu film damage was studied by varying: (1) power density (50 W/cm^2, 2 KW/cm^2); (2) percent transmittance of the film at .6328 μm; (3) two-day old film vs. 1-hour old film; (4) exposure time, to power densities of 50 W/cm^2 and 2 KW/cm^2; and (5) by using substrates of glass and of NaCl crystal.

The results indicate that untarnished Cu films had greater resistance to destruction by the CO_2 laser than two-day old Cu films. Progression of the film destruction seems to have been accelerated tarnishing, then evaporation.

NaCl substrates gave the Cu films a greater resistance to destruction than glass substrates. Again, this shows the tendency of the substrate heating to assist in destroying the film.

3.0 Summary

Improvements in reliability and output power of the CO_2 laser have made high power densities available for thin metals film damage studies. These studies

of Au, Al, Ag, Cu, and Inconel have indicated gold to be the most resistant to destruction. This study also indicates a possibility of using Inconel as a recording plate at 10.6μm.

The thin film samples for this report were made by B. Hoppert, R. McMahon and G. Vershay of this laboratory.

SECTION III

Contract Summary 1 September 1967 - 28 February 1970

ARPA Order 306

Contract Nos. N00014-68-C-0190

N00014-68-C-0190 MOD. P001

N00014-68-C-0190 MOD. P002

1.0 General

During all of the two-year contract period routine determinations were made of thin film damage thresholds for Q-switched ruby laser radiation (Spaceray 101C). The major effort was directed toward dielectric films and film combinations, but work was done on metal films as well. During the 2nd half of the contract a CO_2 laser was constructed. Stable operation was obtained at 60 W output for long periods of time. Semi-quantitative observations of the thresholds of Ag, Cu, Al, Au and Inconel films were made with it.

2.0 Damage by a Ruby Laser

The routine method of determining damage thresholds of thin film coatings exposed at normal incidence to Q-switched ruby laser radiation was developed on the previous Contract NONR-4717(00). It is based on the observation that the damage spots in coated samples at the focus of a lens decrease in radius as the incident energy is reduced toward its threshold value.

The effect depends on the finite divergence of the beam from the laser rod. A plot of energy vs. damage radius is extrapolated to zero radius to find the threshold energy in joules. Multiplying this by an instrumental factor yields the damage threshold energy density in joules per cm^2.

Evaporated films of ZnS, TiO_2, ZrO_2, SiO, SiO_2 and MgF_2 were tested. The thresholds lie between the limits 3 J/cm^2 (ZnS) and 50 J/cm^2 (MgF_2). Multilayer film combinations were also tested - antireflection coatings, beam dividers, quarterwave reflecting stacks, etc. - with thresholds having similar values. Most damage resistant appeared to be ZrO_2/MgF_2 coating structure with thresholds in the 30-40 J/cm^2 range.

A unique method for finding the damage resistance of thin metal films was evolved. The metal is coated on the hypotenuse of a totally reflecting prism and subjected to the unfocused laser beam. At threshold the film is completely removed. Measurements of incident and reflected energies enable the heats of sublimation to be obtained, assuming that the destruction of the film is a thermal process. Reasonable values of the heats of sublimation of Ag, Al and Mo films were found, namely 70, 70 and 110 Kcal/mole, vs. the literature values 68, 78 and 160 Kcal/mole, resp., for bulk materials.

3.0 The CO_2 Laser

The 3.5m CO_2 laser was assembled from 35mm ID Corning Pyrex Conical Pipe System units, is water jacketed and mounted on an H beam which is supported on four 10" innertubes. The Brewster windows are O-ring sealed. The tube is pumped continuously with the He, N_2 and CO_2 gases regulated individually. The discharge is excited by a 20 KV, 150m A (Maximum) regulated DC power supply. The optical cavity is 4m in length. At 60 W multimode output, power densities of 2.2 KW/cm^2 are obtained at the focus of a $f = 10cm$ mirror.

Semi-transparent Au films on NaCl substraces were not damaged by power densities of 1.3 KW/cm^2, but on KBr, BaF_2 and glass the substrate cracked at this level. Clean and fresh Ag films withstood a power density of 2.2 KW/cm^2 for only 1 minute while if dirty they damaged much more easily. Opaque Al films were destroyed at 50 W/cm^2. Cu films appeared to undergo accelerated tarnishing before destruction.

Contrary to the behavior of the above metals, semi-transparent Inconel films reacted to the laser beam cumulatively with a continuous decrease in optical

density, a just perceptible change occurring in a few seconds at a power density level of 50 W/cm^2. They offer some promise for photographic recording at 10.6 μm.

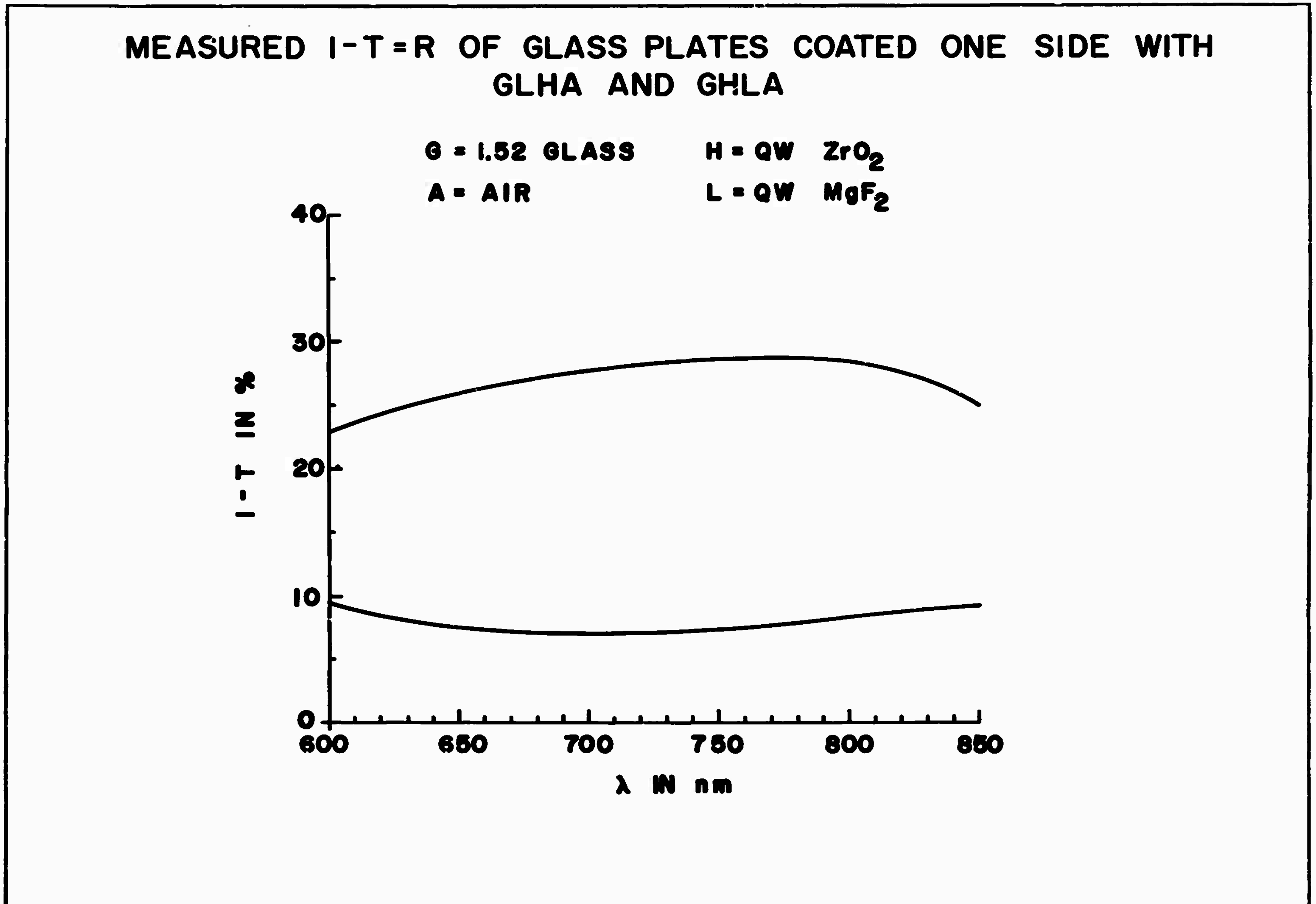
MEASURED 1-T=R OF GLASS PLATES COATED ONE SIDE WITH GLHA AND GHLA
G = 1.52 GLASS
A = AIR
H = QW ZrO2
L = QW MgF2
1-T IN %
40
30
20
10
0
600
650
700
750
800
850
λ IN nm

FIG. 1

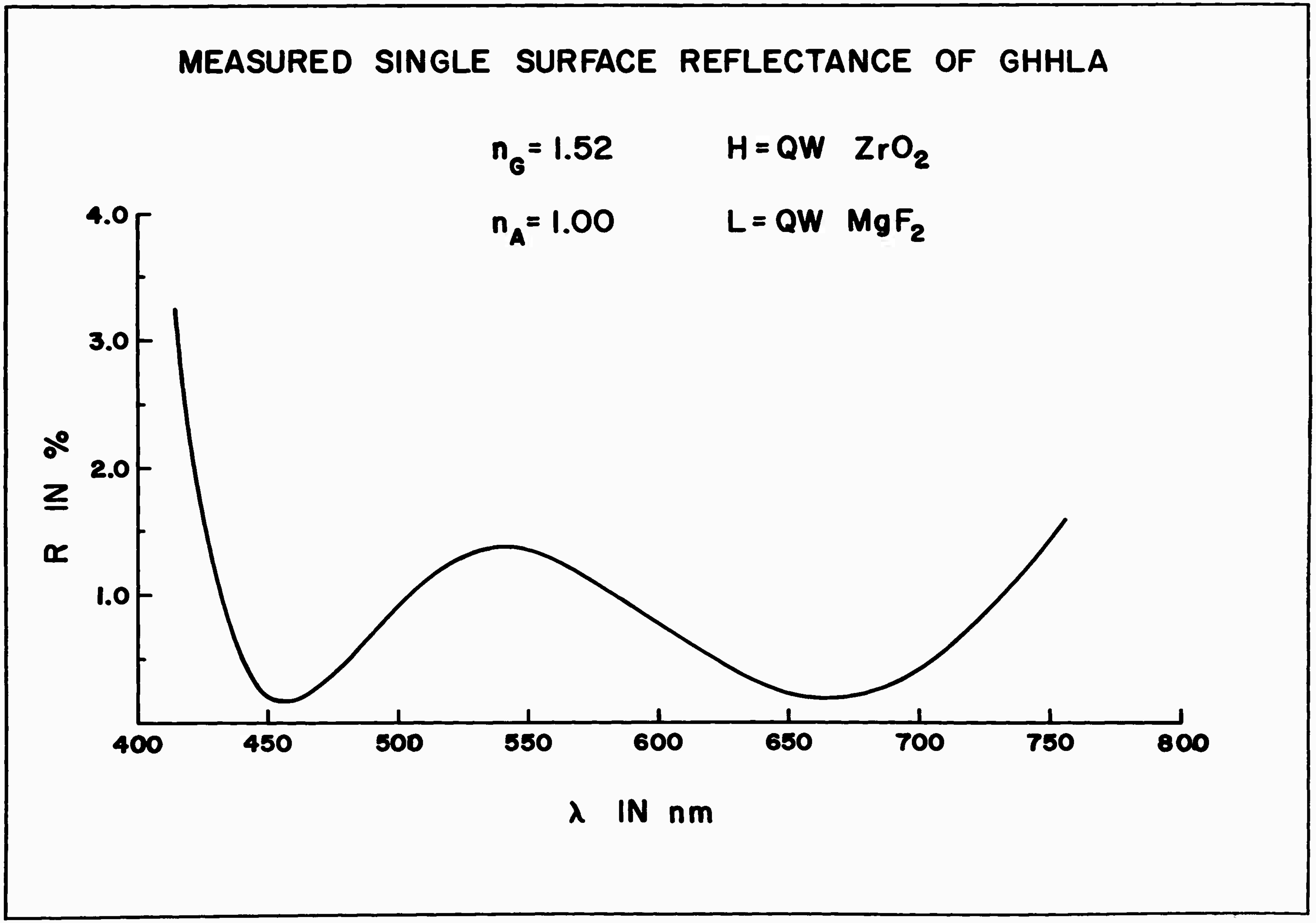

MEASURED SINGLE SURFACE REFLECTANCE OF GHHLA
n_G = 1.52
n_A = 1.00
H = QW ZrO_2
L = QW MgF_2
R IN %
4.0
3.0
2.0
1.0
400
450
500
550
600
650
700
750
800
λ IN nm

FIG. 2A

3-16-70

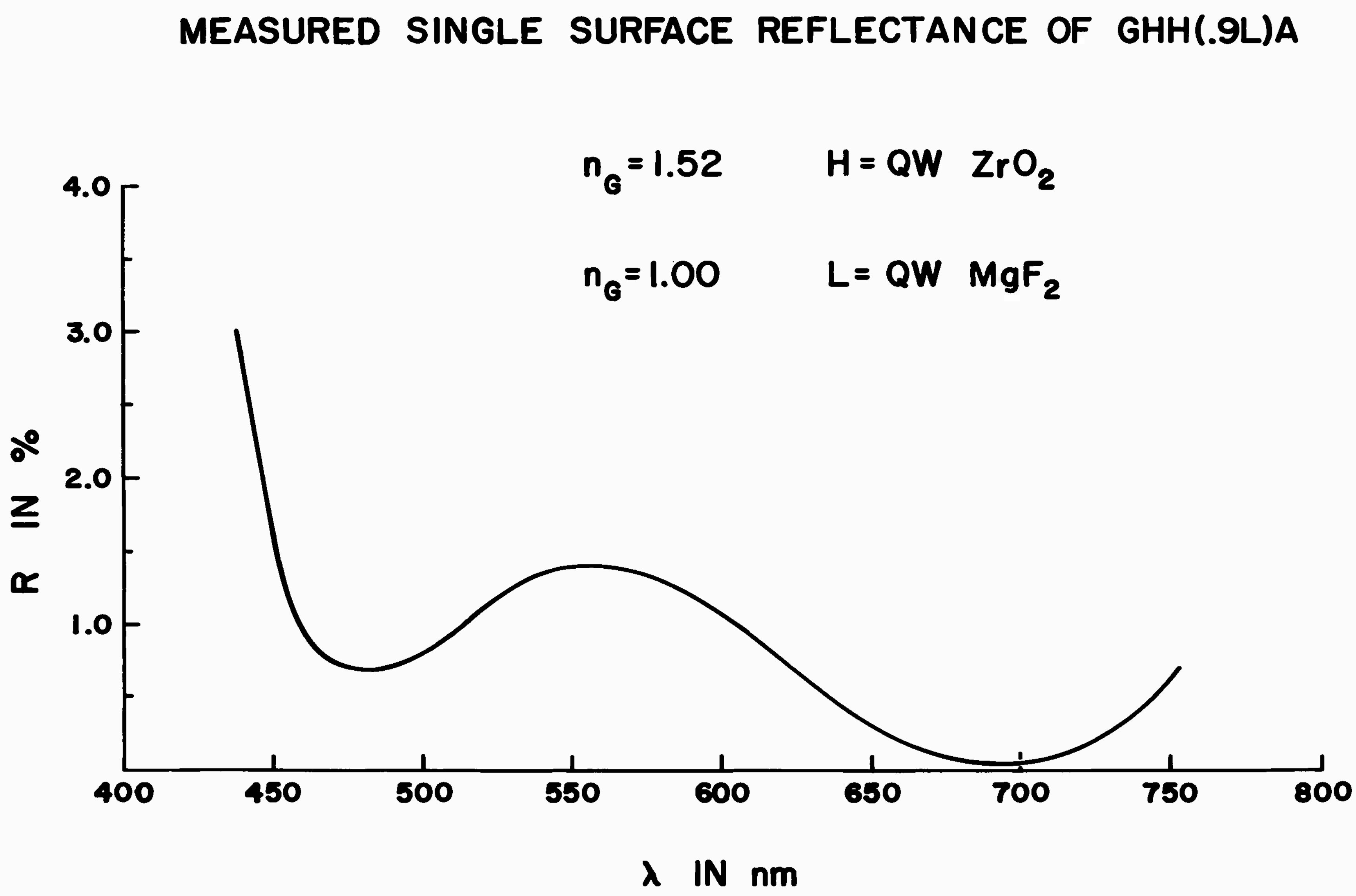

MEASURED SINGLE SURFACE REFLECTANCE OF GHH(.9L)A
n_G = 1.52
H = QW ZrO2
n_G = 1.00
L = QW MgF2
R IN %
4.0
3.0
2.0
1.0
400
450
500
550
600
650
700
750
800
λ IN nm

FIG. 2B

3-16-70

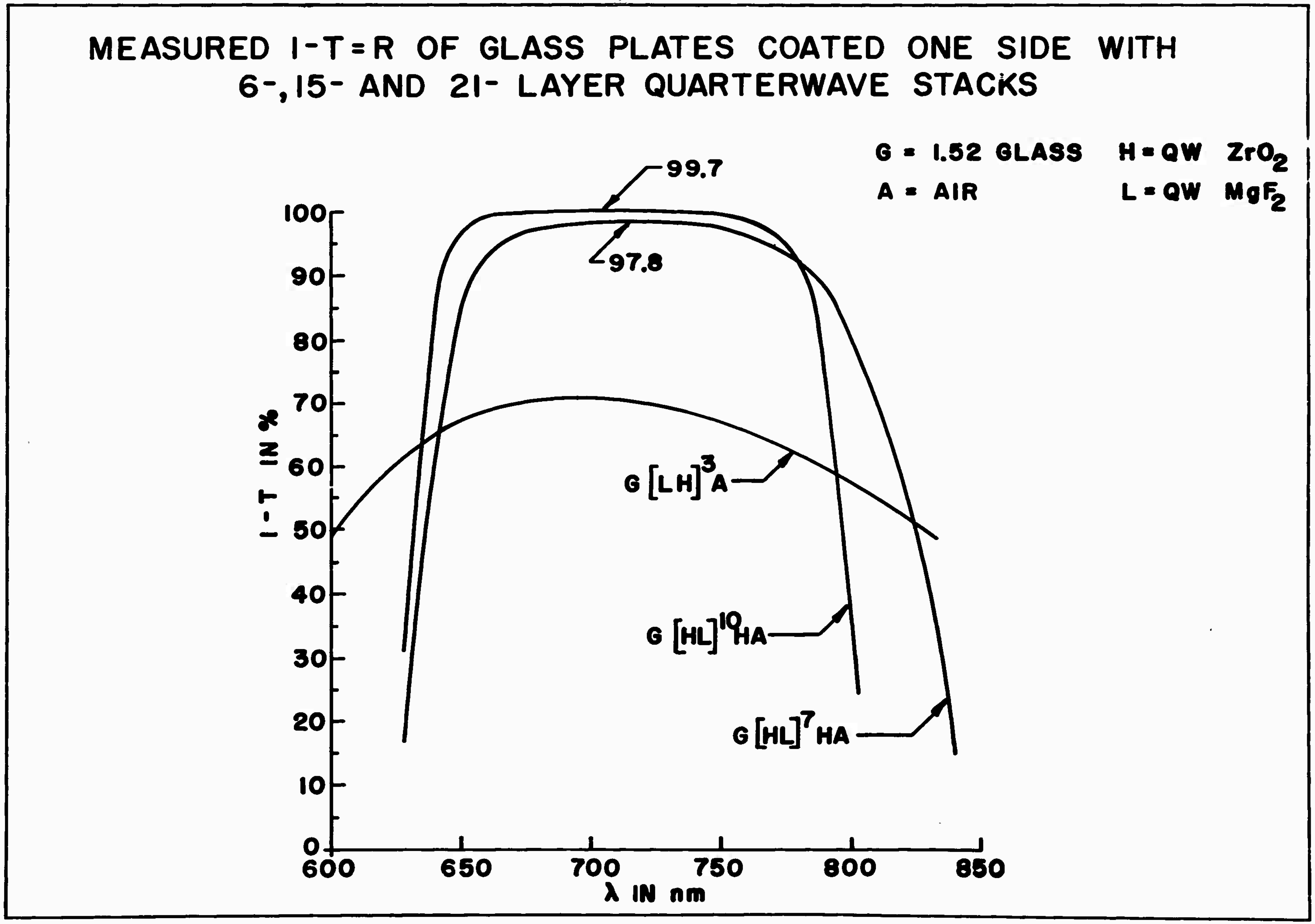
MEASURED 1-T=R OF GLASS PLATES COATED ONE SIDE WITH
6-, 15- AND 21- LAYER QUARTERWAVE STACKS
G = 1.52 GLASS
A = AIR
H = QW ZrO_2
L = QW MgF_2
99.7
97.8
$G[LH]^3A$
$G[HL]^{10}HA$
$G[HL]^7HA$
1-T IN %
100
90
80
70
60
50
40
30
20
10
0
600
650
700
750
800
850
λ IN nm

FIG. 3

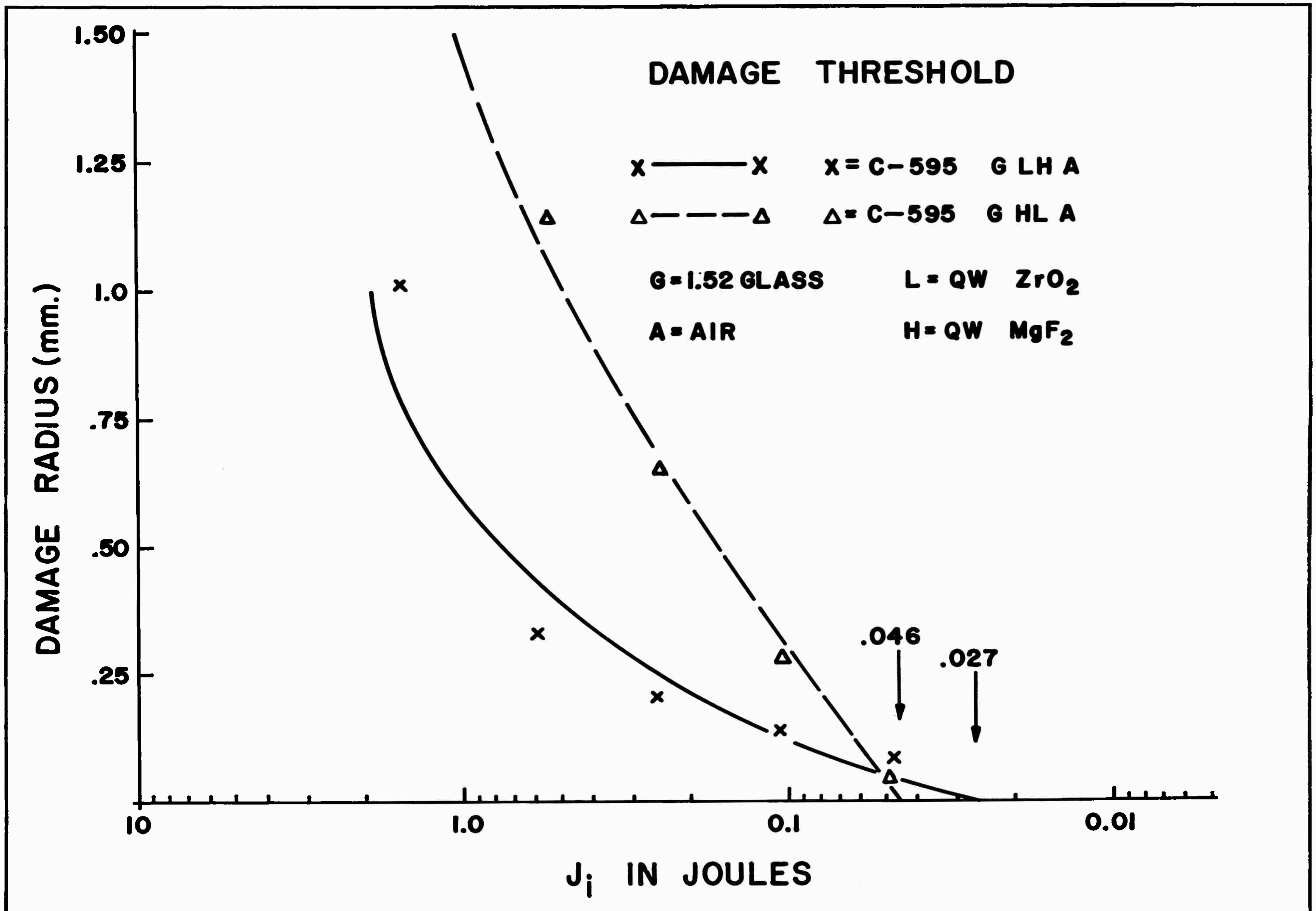

DAMAGE THRESHOLD
X——X X = C-595 G LH A
Δ— — —Δ Δ = C-595 G HL A
G = 1.52 GLASS
L = QW ZrO2
A = AIR
H = QW MgF2
.046
.027
DAMAGE RADIUS (mm.)
1.50
1.25
1.0
.75
.50
.25
10
1.0
0.1
0.01
Ji IN JOULES

FIG. 4

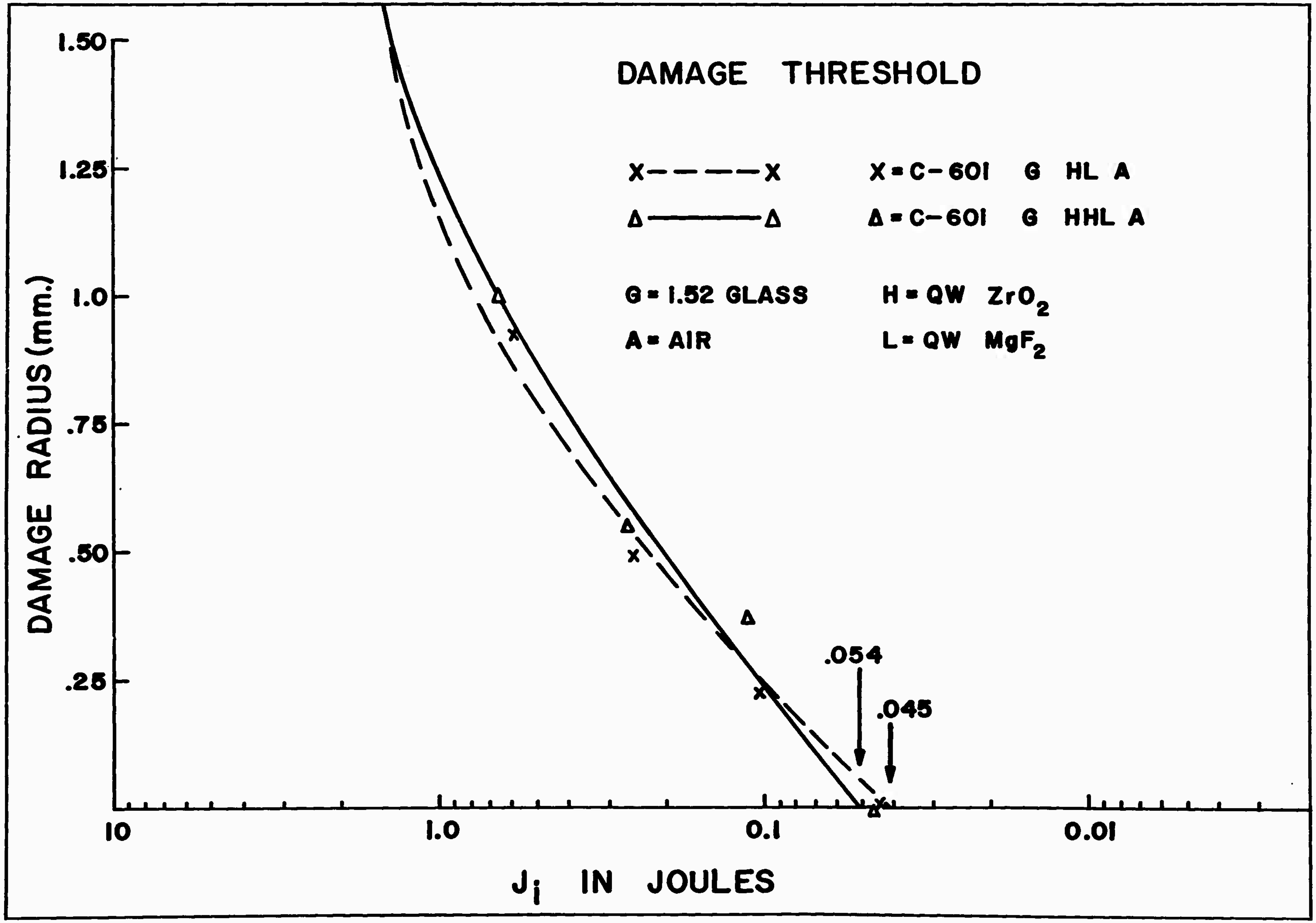
DAMAGE THRESHOLD
X— — — —X
Δ————Δ
X = C-601 G HL A
Δ = C-601 G HHL A
G = 1.52 GLASS
A = AIR
H = QW ZrO_2
L = QW MgF_2
.054
.045
1.50
1.25
1.0
.75
.50
.25
DAMAGE RADIUS (mm.)
10
1.0
0.1
0.01
J_i IN JOULES

FIG. 5

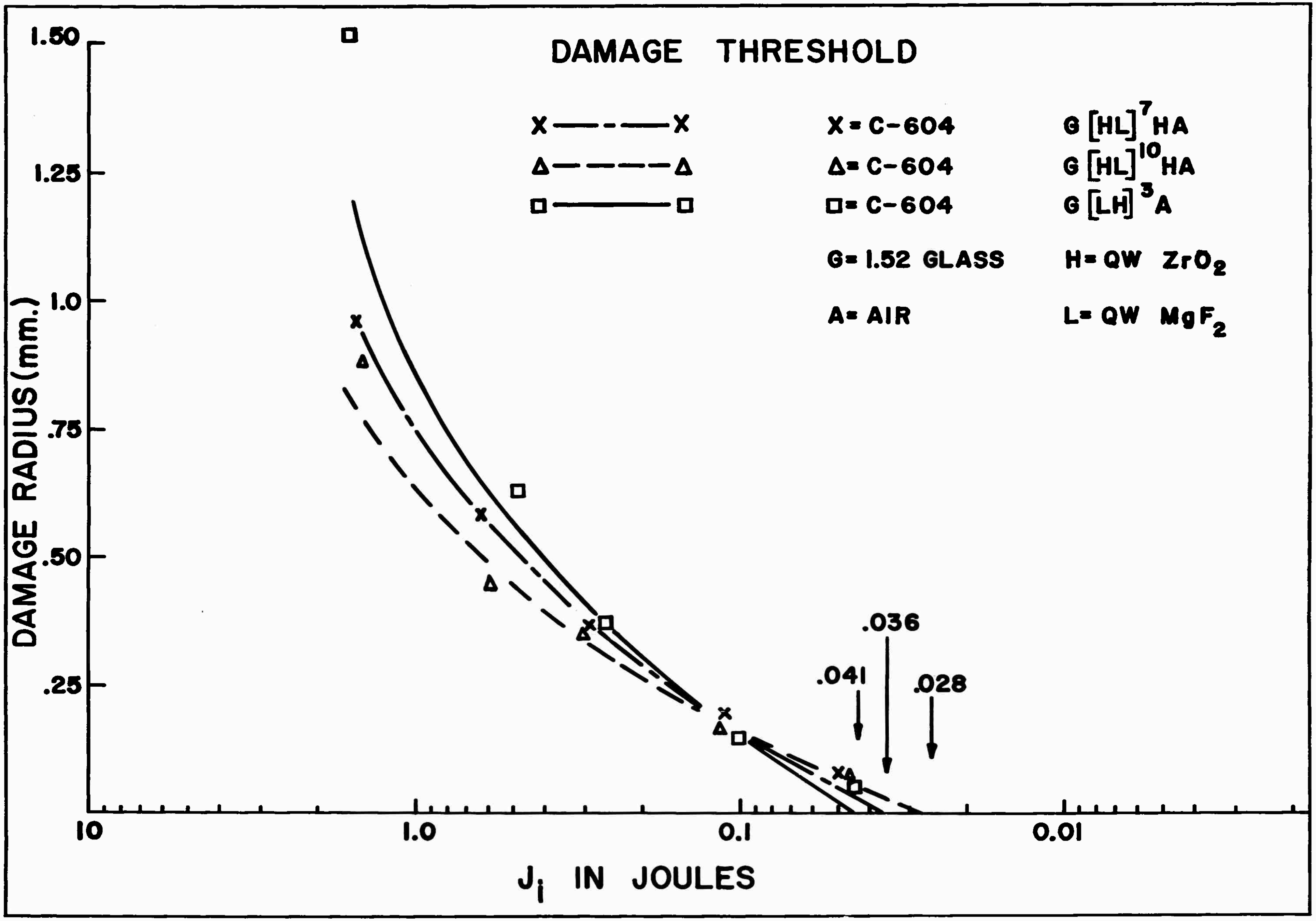
DAMAGE THRESHOLD
X = C-604 G [HL]7 HA
Δ = C-604 G [HL]10 HA
□ = C-604 G [LH]3 A
G = 1.52 GLASS
H = QW ZrO2
A = AIR
L = QW MgF2
.041
.036
.028
1.50
1.25
1.0
.75
.50
.25
DAMAGE RADIUS (mm.)
10
1.0
0.1
0.01
Ji IN JOULES

FIG. 6

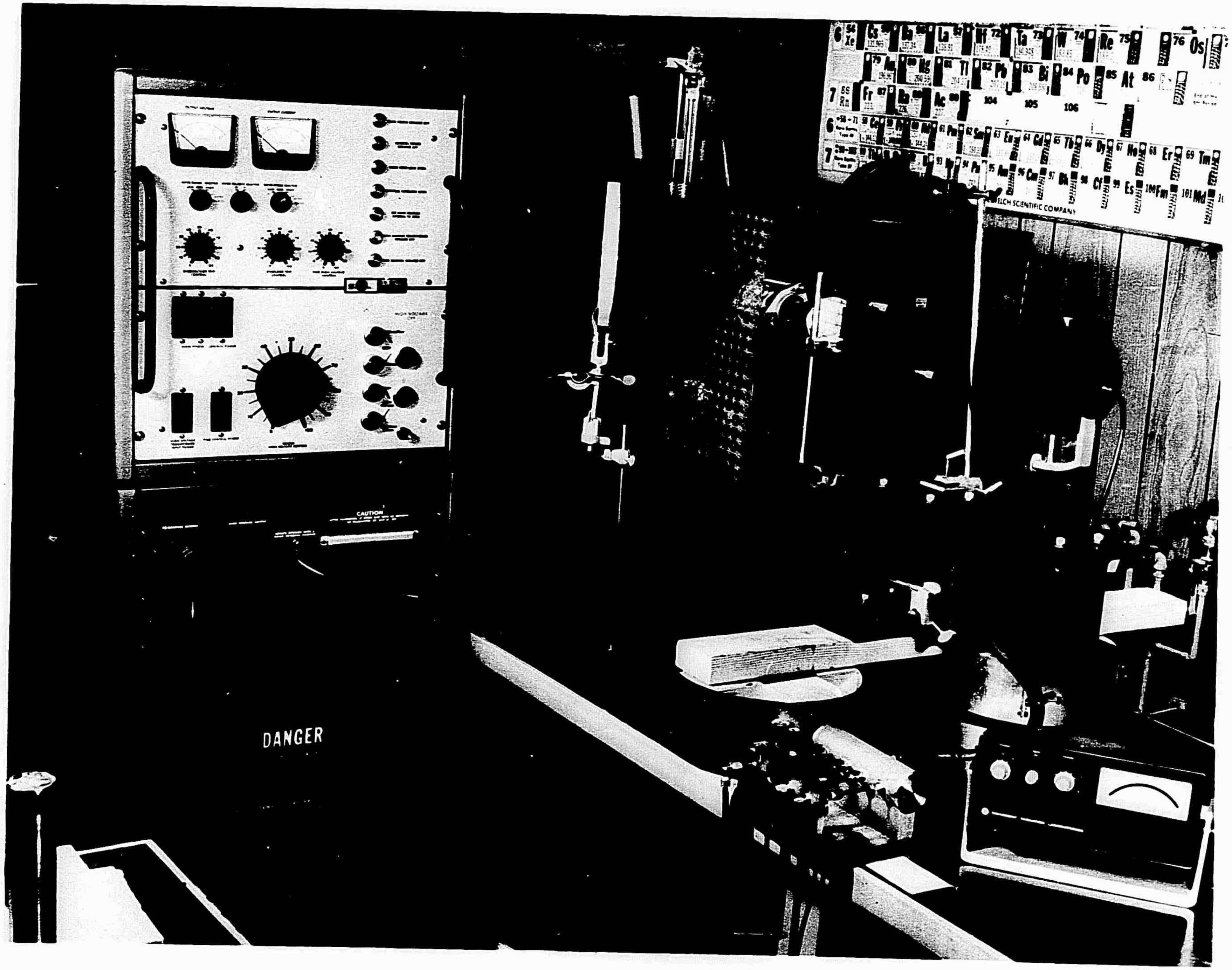

FIG. 7

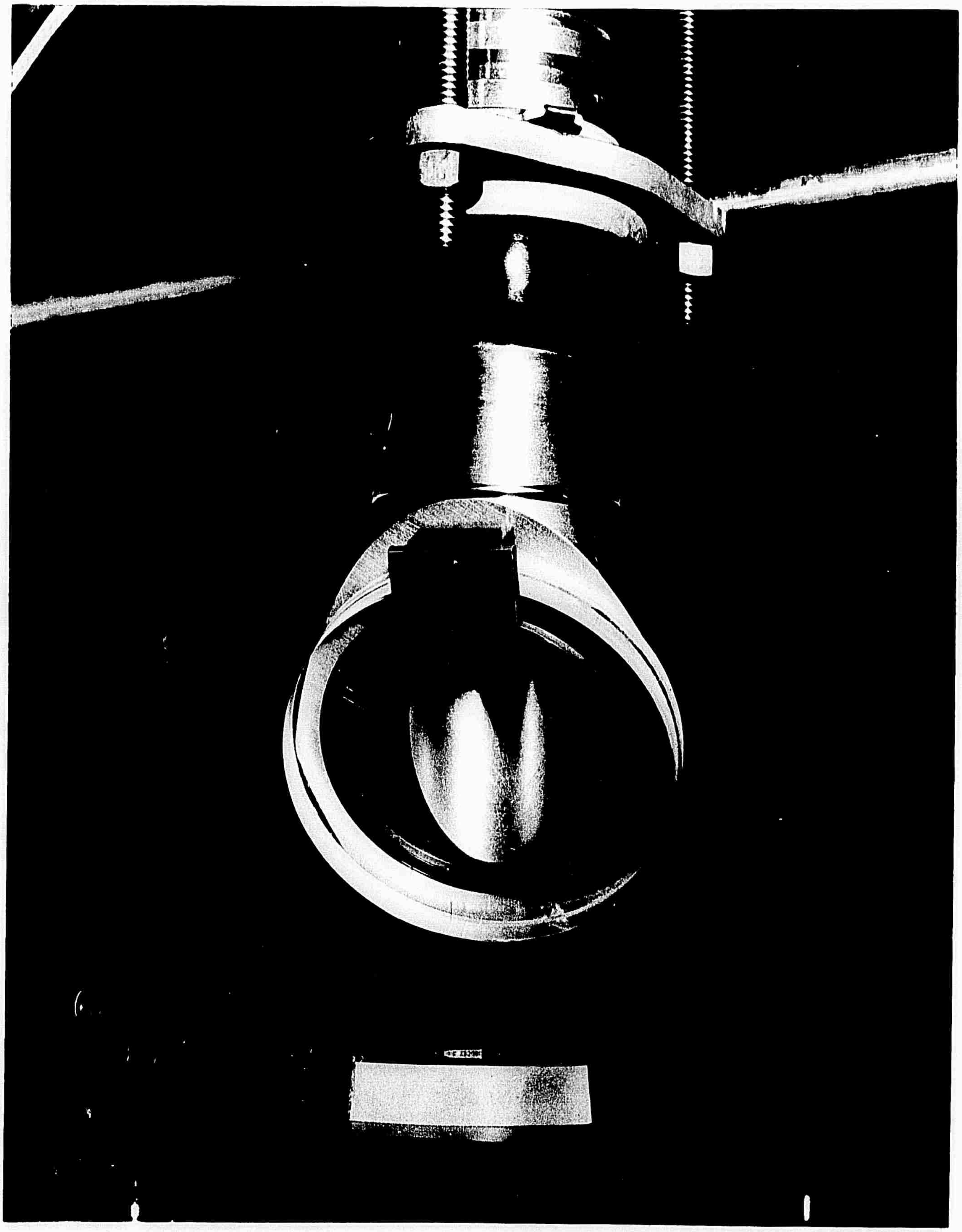

FIG. 8

CALCULATED R AND T OF SILVER FILMS VS. THICKNESS IN ANGSTROMS AT $\lambda = 0.6328\mu m$ AND $10.6\mu m$. SUBSTRATE INDEX 1.52

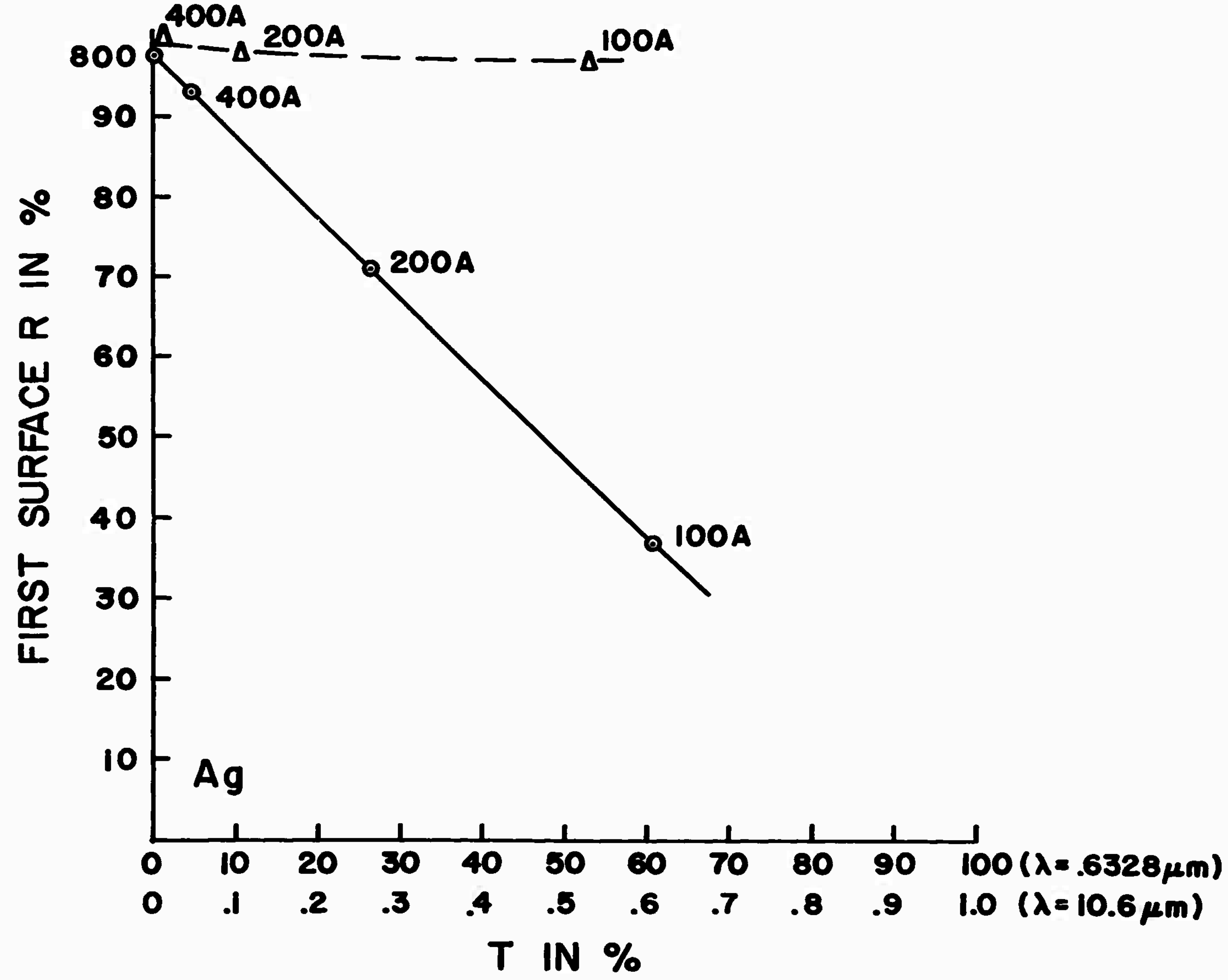

FIG. 9

12-23-69

CALCULATED R AND T OF COPPER FILMS VS. THICKNESS IN ANGSTROMS

AT $\lambda = 0.6328 \mu m$ AND $10.6 \mu m$. SUBSTRATE INDEX 1.52

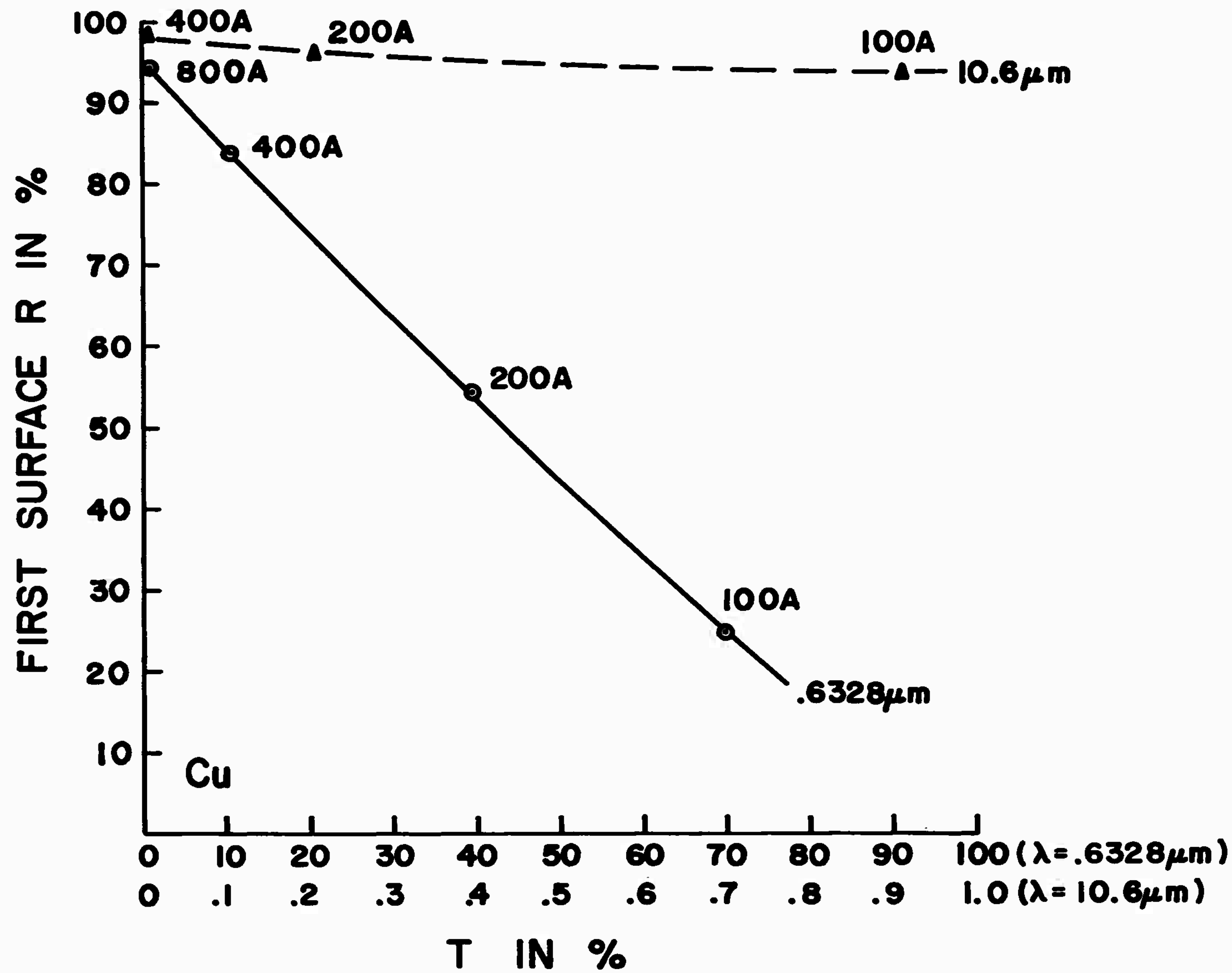

FIG. 10

3-16-70

CALCULATED R AND T OF ALUMINUM FILMS VS. THICKNESS IN ANGSTROMS
AT λ=0.6328μm AND 10.6μm. SUBSTRATE INDEX 1.52

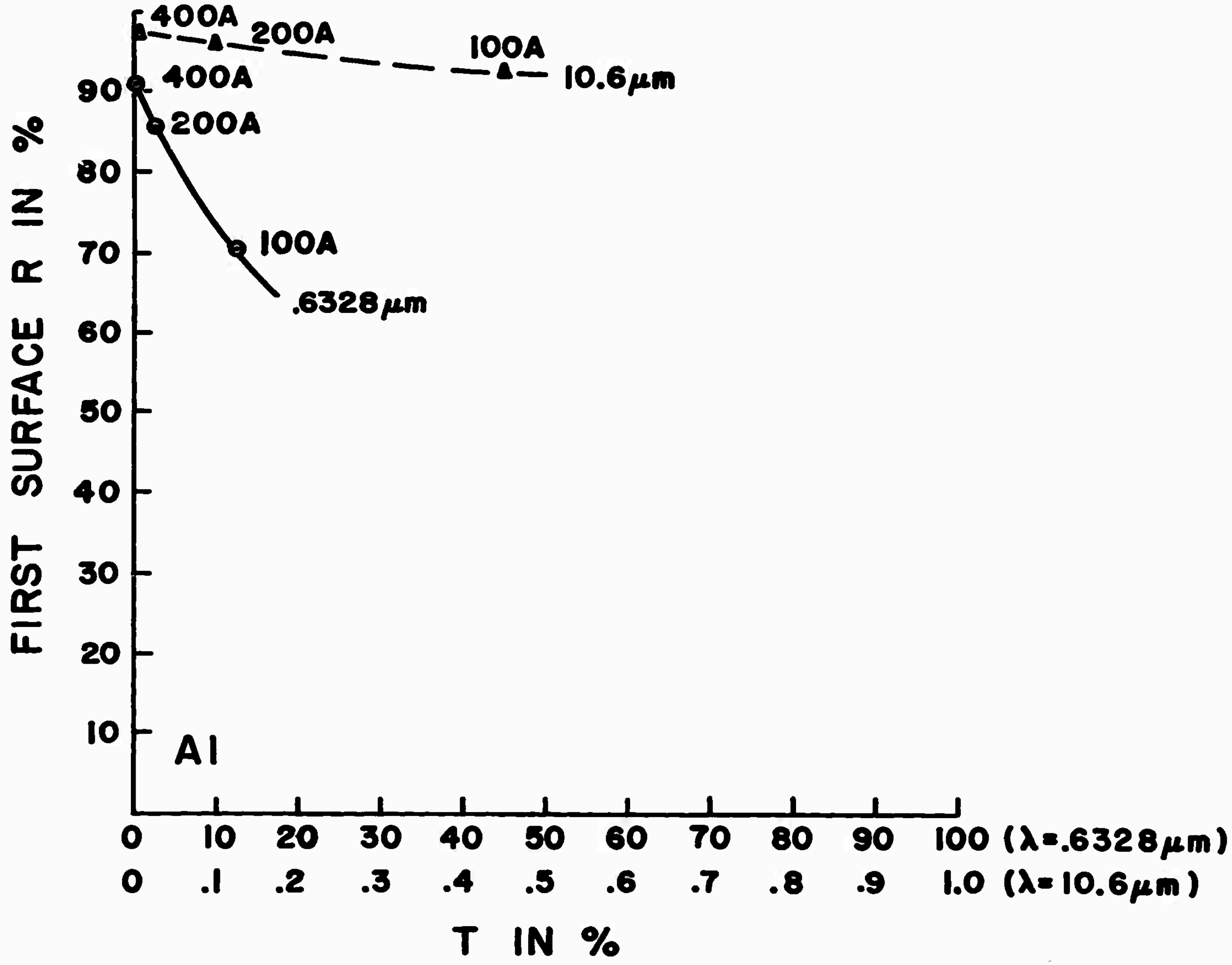

FIG. 11

12-23-69

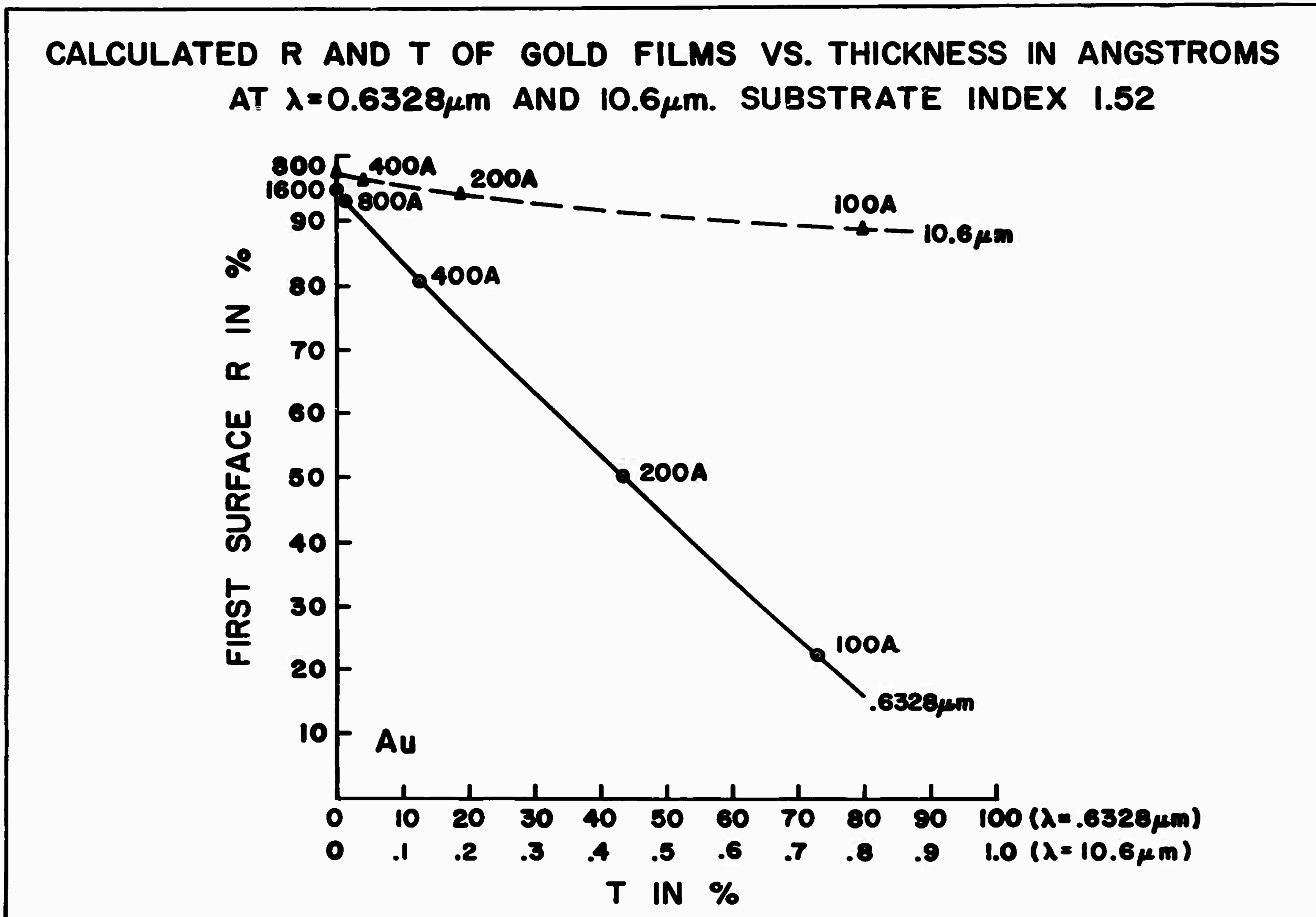

FIG. 12

12-23-69

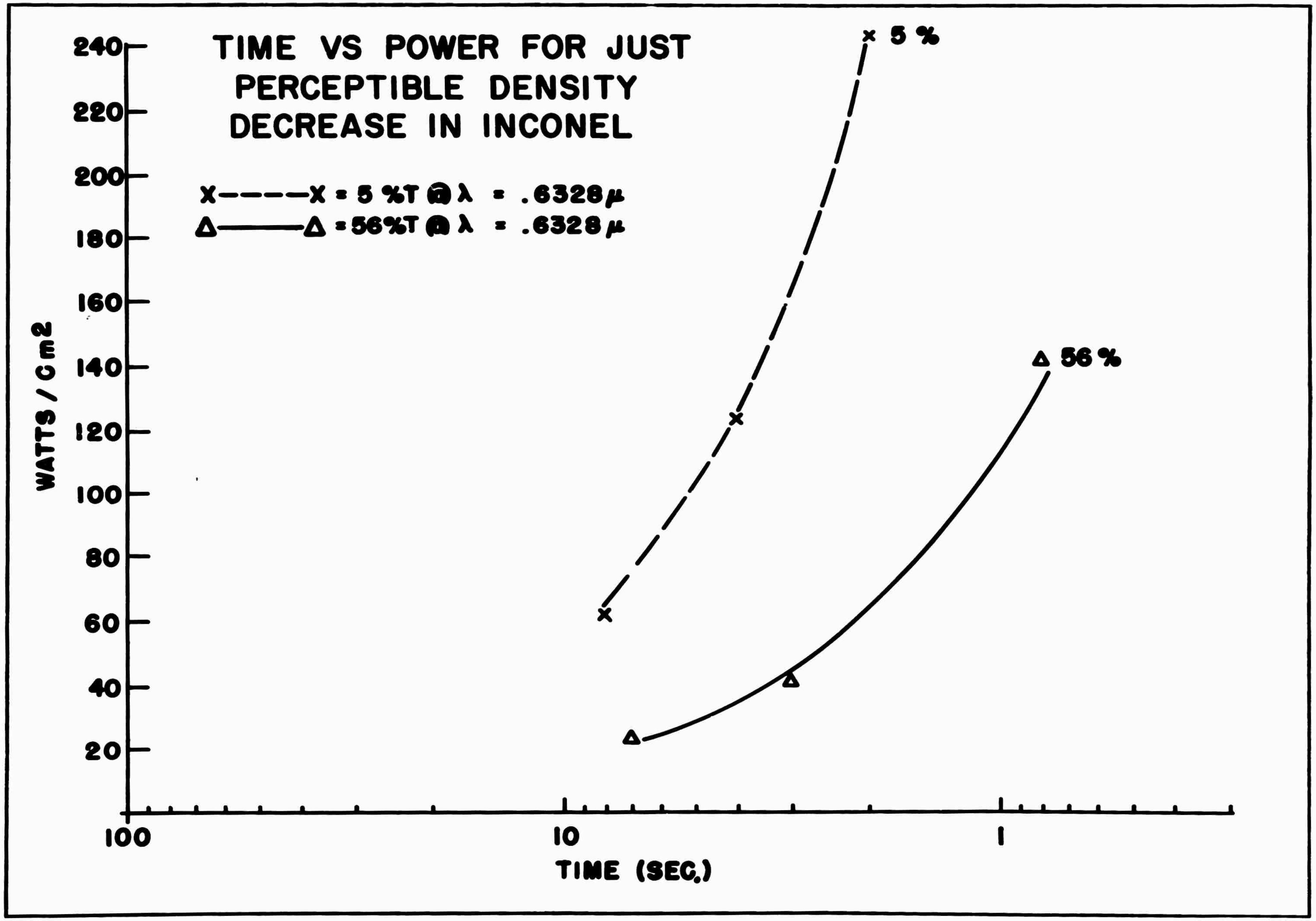

TIME VS POWER FOR JUST PERCEPTIBLE DENSITY DECREASE IN INCONEL
X-----X = 5 %T @ λ = .6328 μ
Δ——Δ = 56%T @ λ = .6328 μ
× 5 %
Δ 56 %
WATTS / Cm2
240
220
200
180
160
140
120
100
80
60
40
20
100
10
1
TIME (SEC.)

FIG. 13

BLANK PAGE

Security Classification

DOCUMENT CONTROL DATA - R & D

(Security classification of title, body of abstract and indexing annotation must be entered when the overall report is classified)

1. ORIGINATING ACTIVITY (Corporate author) Bausch & Lomb Incorporated Rochester, New York 14602	2a. REPORT SECURITY CLASSIFICATION Unclassified 2b. GROUP

3. REPORT TITLE

Laser Damage Study of Thin Films

4. DESCRIPTIVE NOTES (Type of report and inclusive dates)

Eighth and Final Quarterly Report 29 November 1969 to 28 February 1970

5. AUTHOR(S) (First name, middle initial, last name)

Arthur F. Turner Edward M. Arlin

6. REPORT DATE	7a. TOTAL NO. OF PAGES	7b. NO. OF REFS
28 February 1970	27	0

8a. CONTRACT OR GRANT NO. N00014-68-C-0190 MOD. P002 b. PROJECT NO. ARPA Order 306 c. d.	9a. ORIGINATOR'S REPORT NUMBER(S) Eighth and Final Quarterly Report 28 February 1970 9b. OTHER REPORT NO(S) (Any other numbers that may be assigned this report)

10. DISTRIBUTION STATEMENT

1

11. SUPPLEMENTARY NOTES	12. SPONSORING MILITARY ACTIVITY Office of Naval Research Physics Branch Washington, D. C. 20360 Attn: Mr. F. B. Isakson Head, Physics Branch

13. ABSTRACT

Damage thresholds for evaporated ZrO_2 films and multilayers, in combination with MgF_2 films, were determined using a Q-switched ruby laser. Antireflection and beam divider coatings as well as high reflecting quarterwave stacks were represented in the multilayers tested. Threshold values lie in the 30-40 J/cm^2 range for coatings with up to 15 layers. Beyond this the thresholds decrease. The CO_2 laser assembled here was improved by introducing O-ring seals for the Brewster windows and by more efficient water cooling. It is stable at 60 W multimode for periods of hours. Semi-quantitative observations were made on metal films of several thicknesses - Ag, Cu, Al, Au and Inconel. Au appears most damage resistant. Inconel films show promise for photographic recording at 10.6 μm.

DD FORM 1473 1 NOV 65

Unclassified

Security Classification

Security Classification

14. KEY WORDS	LINK A		LINK B		LINK C	
	ROLE	WT	ROLE	WT	ROLE	WT
Laser damage; thin films; ruby; CO_2						

Unclassified

Security Classification